

Prevalence of first-order kinetics in thermoluminescence materials: An explanation based on multiple competition processes

Vasilis Pagonis^{*1} and George Kitis²

¹Physics Department, McDaniel College, Westminster, MD 21157, USA

²Nuclear Physics Laboratory, Aristotle University of Thessaloniki, 54124 Thessaloniki, Greece

Received 28 November 2011, revised 15 February 2012, accepted 21 February 2012

Published online 19 March 2012

Keywords first-order kinetics, kinetic modeling, thermoluminescence

* Corresponding author: e-mail vpagonis@mcdaniel.edu, Phone: +001 410 857 2481, Fax: +001 410 386 4624

Typical materials used in thermoluminescence (TL) dosimetry exhibit the following common characteristics: (i) the temperature of glow peak maximum of individual glow peaks remains practically constant over a wide dose range, (ii) there are no systematic changes in the glow curve shapes with the irradiation dose, and (iii) higher order kinetics is rarely seen in dosimetric materials, while first-order kinetics is a common occurrence in experimental TL work. Theoretical explanation of these experimental characteristics is an open topic of TL research. In the present work these three characteristics are studied by using several models of increasing complexity. The simplest model studied is based on the empirical analytical general order (GO) expressions, followed by two commonly used models, the well-known one trap one recombination center models (OTOR) and the interactive multiple trap system (IMTS). Previous researchers have studied the behavior of these models using arbitrary values of the kinetic parameters in the models, and by varying these parameters within limited physically reasonable ranges. In this paper, a new method of analyzing the results from such

models is presented, in which the average behavior of real dosimetric materials is simulated by allowing simultaneous random variations of the kinetic parameters, within several orders of magnitude. The simulation results lead to the conclusion that the presence of many competitive processes during the heating stage of TL, may be correlated to the remarkable stability of the glow curve shapes exhibited by most materials, and to the prevalence of first-order kinetics. This correlation is demonstrated further by a series of simulations in which the number of competitor traps is increased systematically, by adding up to 12 competitor traps in the IMTS model. As the number of competitor traps increases, the average behavior of the TL glow curves tends progressively toward first-order kinetics, and this in turn results in very small average variations in the shape of the TL glow peak. The simulation results in this paper provide a convincing demonstration and explanation of the stability of the shape of TL glow curves in dosimetric materials, and for the prevalence of first-order kinetics in TL.

© 2012 WILEY-VCH Verlag GmbH & Co. KGaA, Weinheim

1 Introduction Typical thermoluminescence (TL) materials used in dosimetry show the following common characteristics [1–3]:

- (i) The temperature of glow peak maximum T_{\max} of individual glow peaks remains practically constant, over a wide range of irradiation doses.
- (ii) There are no systematic changes in the glow curve shape, even when the irradiation dose is changed over several orders of magnitude.

(iii) First-order kinetics is a common occurrence in experimental TL work [4] while higher order kinetics is rarely seen in dosimetric materials.

Theoretical explanation of these experimental characteristics is an open topic of TL research. From its early history [5, 6], TL theory has predicted the shift of T_{\max} as a function of the heating rate used during TL experiments, and also as a function of the irradiation dose. The shift of T_{\max} due to the heating rate is a common experimental

characteristic of all dosimetric materials, and has been the basis of a rich literature on the evaluation of trapping parameters [5, 7–13]. However, there are few experimental results showing complete TL glow peaks fitted quantitatively with general order (GO) kinetic expressions at different doses, and which follow exactly the theoretical pattern of GO kinetics.

The simplest phenomenological model describing a single TL glow peak, consists of one trap and one recombination center (OTOR model) [12]. Additional kinetic models have been suggested, which take into account multiple electron traps and recombination centers. The basic representatives of such models are the interactive multiple trap system (IMTS) and non-interactive multitrapping system (NMTS) models [12]. In addition to the main active dosimetric trap, these models contain thermally disconnected deep traps (TDDT). These TDDT are considered to be thermally stable during the TL experiment.

Previous researchers have studied the behavior of these models using arbitrary values of the kinetic parameters in the models, and by varying these parameters within reasonable but rather limited physical ranges. For instance, Sunta et al. [2, 3] found that the TL glow curves produced by the OTOR and general order kinetics (GOK) models do not agree with the above listed properties of experimental glow curves.

The theoretical location of T_{\max} and the shape of the glow curves in these models undergo a systematic change with the irradiation dose, and the glow curve area varies in most cases linearly with the initial occupancy of the traps. By contrast, these authors proposed that glow peaks calculated using the IMTS model, exhibited the same TL glow curve shape at all trap occupancies, and the intensity grew supralinearly with the trap occupancy. The aims of the present work are:

- To carry out a comprehensive simulation of these dosimetric properties, using both analytical TL expressions and kinetic models of increasing complexity.
- To investigate possible reasons for the prevalence of first-order kinetics in most TL dosimetric materials.
- To make clear the discrepancies between the predictions of the models and the experimental results.
- To demonstrate how the presence of multiple competition processes in real dosimetric materials, can lead to the remarkable stability of the shape of TL glow peaks, and to the prevalence of first-order kinetics.

In the present work dosimetric characteristics are studied by using several different models, with increasing complexity. The simplest models are based on the empirical analytical GO expression. Next, the commonly used OTOR and IMTS models are studied, and the results are compared with previous studies [2, 3]. The average behavior of real dosimetric materials is simulated using a new technique of analyzing the results from the models, by allowing wide random variations of the kinetic parameters within several orders of magnitude. The overall results from the IMTS

model show that the presence of many competitive processes during the TL heating stage is correlated to the remarkable stability of the TL glow curves in real dosimetric materials. This correlation is demonstrated further by a series of simulations, in which the number of competitor traps is increased systematically, by adding up to 12 thermally disconnected competitor traps to the IMTS model. The results show that as the number of competitor traps increases, the average behavior of the TL glow curves tends toward first-order kinetics, and this in turn results in systematically smaller average variations in the shape of the TL glow peak. Specifically, it is found that random variations of the parameters in the model within many orders of magnitude, produce very small average variations in the shape of the TL glow peak, in the apparent kinetic order b , and in the value of T_{\max} .

Overall, the simulations in this paper provide a convincing demonstration of the importance of multiple competition processes in determining the remarkably stable shape of TL glow curves in dosimetric materials. Furthermore, the simulated results provide an explanation for the prevalence of first-order kinetics in TL materials, based on the presence of multiple competition processes during the heating stage of TL.

It is noted that in this paper the term “first-order kinetics TL peaks” is used to describe asymmetric peaks with a symmetry factor of 0.42, regardless of the underlying physical mechanism. Strictly speaking, this terminology should be used only for peaks generated from the real first-order kinetic model of Randall and Wilkins [5]. More complex situations and kinetics, such as the OTOR and IMTS models in this paper, can lead to TL peaks with shape and geometry similar to first-order TL glow peaks. However, the term “first-order kinetics TL peaks” is widely used in the TL literature to describe the TL peaks in the OTOR and IMTS models, and is also used in this paper.

2 Numerical simulation of T_{\max} shift The TL theory based on first-order kinetics predicts that the shape of TL glow curves remains the same, independently of the irradiation dose received by the sample. Specifically the shape of first-order TL glow curves is asymmetric, and is characterized by a value of the geometrical shape factor $\mu_g = \delta/\omega = 0.42$ [12]. This prediction is in agreement with the behavior of most commonly used dosimetric TL materials.

However, empirical analytical expressions describing second and GO TL kinetics predict a change of the shape of TL glow curves, as well as a shift of T_{\max} with the irradiation dose [5, 6, 14, 15]. The analytical expression for the empirical GO kinetics equation is [15]:

$$I(T) = s \frac{n_0^b}{N^{b-1}} \exp\left(-\frac{E}{kT}\right) \times \left[1 + \frac{s(b-1)}{\beta} \left(\frac{n_0}{N}\right)^{b-1} \int_{T_0}^T \exp\left(-\frac{E}{kT'}\right) dT'\right]^{-\frac{b}{b-1}}, \quad (1)$$

where b is the kinetic order parameter, E (eV) the activation energy of the trap, n_o (cm^{-3}) the initial trap occupancy, T (K) the sample temperature, N (cm^{-3}) the total trap concentration, s (s^{-1}) the frequency factor for the trap, and T_o (K) is the room temperature. It is noted that in the above analytical GO equation, the effect of the irradiation dose is expressed via the ratio n_o/N , which represents the initial degree of filling of the dosimetric traps at the start of the TL heating stage. This empirical analytical equation contains a total of five parameters E , s , b , n_o and N .

Previous work [2, 3] has shown that the empirical GO kinetics analytical Eq. (1), predicts a change in the shape of the TL glow curves, a shift of T_{max} with dose, and a variation of the kinetic parameter b with the irradiation dose. These theoretical predictions from the empirical analytical GO expression, are in disagreement with the experimental behavior of most dosimetric materials [21].

In this paper, simulations are carried out with two commonly used general models of TL, namely the OTOR and IMTS kinetic models. The IMTS model contains two traps and one recombination center [2, 3, 16]. The differential equations governing the traffic of electrons between the two trapping levels, the recombination center, and the conduction band in the IMTS model are:

$$\frac{dT}{dt} = \beta, \quad (2)$$

$$\frac{dn_c}{dt} = -\frac{dn_1}{dt} - \frac{dn_2}{dt} - n_c mA_m, \quad (3)$$

$$\frac{dn_1}{dt} = -n_1 s \exp\left(\frac{-E}{kT}\right) + n_c(N_1 - n_1)A_n, \quad (4)$$

$$\frac{dn_2}{dt} = n_c(N_2 - n_2)A_d, \quad (5)$$

$$I(t) = -\frac{dm}{dt} = n_c mA_m, \quad (6)$$

The charge neutrality, which dictates that

$$m = n_1 + n_2 + n_c \quad (7)$$

is also included in the above set of differential equations. Equation (2) accounts for the linear increase of temperature with a heating rate β (K/s). In the above equations, N_1 and N_2 (cm^{-3}) are the total concentrations of the dosimetric and competitor electron traps in the crystal, and $n_1(t)$, $n_2(t)$ (cm^{-3}) are the corresponding instantaneous concentrations of filled traps. n_c (cm^{-3}) is the instantaneous concentration of free carriers in the conduction band, m (cm^{-3}) the concentration of recombination centers in the crystal, A_n (cm^3/s) the capture coefficient for the dosimetric traps, A_m (cm^3/s) the capture coefficient of the recombination center, and A_d (cm^3/s) is the capture coefficient of the competitor trap. E (eV) is the activation energy of the dosimetric traps, s (s^{-1}) the frequency factor for this trap, k (eV/K) the

Boltzmann constant, β (K/s) the constant heating rate, t (s) the time, and T (K) is the temperature of the sample.

The initial concentrations of the two traps in the IMTS model at time $t=0$ are denoted by the symbols n_{10} and n_{20} correspondingly. In this paper, the heating stage of TL is simulated, while the effect of the prior irradiation dose is studied by varying the initial concentration of the dosimetric trap filling n_{10} . The prior irradiation dose D can be assumed under certain conditions to be proportional to the initial dosimetric trap filling n_{10} . As discussed later in the paper, a more complete method of simulating the behavior of dosimetric materials is by carrying out simulations for both the excitation and the heating stage of TL.

The IMTS model presents an additional level of complexity over the analytical GO model discussed above, since it contains explicitly the effect of competition during heating, by including the three recombination/retrapping coefficients A_m , A_n , A_d . In total, the IMTS model contains nine parameters, namely E , s , A_m , A_n , A_d , N_1 , N_2 , n_{10} , and n_{20} .

In the present simulations the following numerical values are used for the parameters, unless indicated otherwise: A_m , A_n , $A_d = 10^{-7} \text{ cm}^3/\text{s}$, $N_1 = N_2 = 10^{12} \text{ cm}^{-3}$, $\beta = 1 \text{ K/s}$, $E = 1 \text{ eV}$, and $s = 10^{12} \text{ s}^{-1}$. With these values of E , s and β , the value of T_{max} for first-order kinetics is expected to be at $T_{\text{max}} = 385 \text{ K}$. The value of the geometrical shape factor for first-order kinetics is expected to be $\mu_g = \delta/\omega = 0.42$.

The rate Eqs. (2–7) describing the traffic of electrons during the linear heating process, are coupled first-order non-linear differential equations, which unfortunately cannot be solved in close form. The development of analytical expressions for the TL intensity as a function of temperature requires simplifying assumptions, with the most important one being the quasi-equilibrium (QE) conditions.

When the competitor trap is saturated, that is, when $n_{20} = N_2$, the IMTS model is known as the non-interactive multiple trap system (NMTS). On the other hand, in the absence of the competitor trap (i.e., when $N_2 = 0$), the IMTS model becomes the OTOR model.

During numerical solution of the differential equations the following quantities are evaluated, which are necessary for this study:

- (i) The total peak integral A .
- (ii) The peak maximum intensity I_{max} .
- (iii) The peak maximum temperature T_{max} and the temperatures T_1 and T_2 at the half maximum intensity $I_{\text{max}}/2$, at the low and high temperature part of the glow-peak, respectively.
- (iv) The full width at half maximum $\omega = T_2 - T_1$, and the half widths $\tau = T_m - T_1$ and $\delta = T_2 - T_m$.
- (v) The geometrical symmetry factor $\mu_g = \delta/\omega$ and the integral symmetry factor $\mu'_g = (\text{integral from } T_{\text{max}} \text{ to } T_{\text{infinity}}) / (\text{total peak integral})$.
- (vi) The triangle assumption pseudo-constants C_ω , C_τ , and C_δ [12, 17, 18], which represent the degree by which a single TL glow peak is approximated by a

triangle. These constants are the basis for the peak shape methods of evaluating of activation energy. For example, the quantity C_ω is the triangle assumption pseudo-constant, which expresses the degree by which a TL peak approaches the shape of a triangle. This constant is easily evaluated during the simulation by the relation [17, 18]

$$C_\omega = \frac{\omega I_{\max}}{\beta A}, \quad (8)$$

where I_{\max} is the peak maximum intensity and A is the total integrated area of the numerically generated TL peak.

Several different methods of analyzing the numerically calculated glow curves are used in this paper, in order to calculate the kinetic order b and the activation energy E . In order to describe the TL glow peaks obtained from the numerical solution of the above differential equations, one commonly fits the numerically generated TL peaks by using the empirical GO Eq. (1). However, in the present work we use two alternative equivalent procedures instead of a TL glow curve fitting procedure, as follows.

In the first method, the value of E is obtained using the well-known Chen peak shape equations [12].

$$E_{\text{gen}} = c_\alpha \frac{kT_{\max}^2}{\alpha} - b_\alpha (2kT_{\max}), \quad (9)$$

where α is τ , δ , or ω . The values of the constants c_α and b_α are calculated using the geometrical shape factor μ_g , which is also used to estimate the kinetic order b [12].

The second method used in this paper is a faster and equally reliable method, based on recently developed peak shape methods for both general and mixed order kinetics [17, 18]. This procedure was used recently to simulate the effect of thermal quenching on the TL glow curves of quartz [19].

Once the integral symmetry factor μ'_g and T_{\max} of each glow-peak is evaluated, then the kinetics order b of the glow-peak can be evaluated using the following iterative equation given by Kitis and Pagonis [18], their Eq. (18):

$$\mu'_g = \left[\frac{b}{1 + (b-1)(2kT_m/E)} \right]^{\frac{1}{b-1}}. \quad (10)$$

Equation (10) relates a TL peak obtained from the numerical solution of Eqs. (2)–(7) having an integral symmetry factor μ'_g , with a TL peak calculated from an analytical GO expression having the same integral symmetry factor. As can be seen from the parameters involved in Eq. (10), the integral symmetry factor μ'_g is a pure kinetic parameter, unlike the well-known geometrical symmetry factor μ_g which is a simple geometrical factor [17, 18, 20].

Having evaluated the kinetic order parameter b as described above, the value of the activation energy E can be

evaluated using the following equation given by Kitis and Pagonis ([18], their Eq. (22)):

$$E_g = C_\omega b \mu'_g \frac{kT_{\max}^2}{\omega}. \quad (11)$$

Equation (11) evaluates the activation energy E based specifically on the shape of the glow peak, and uses the full width at half maximum ω . Similar equations involving τ , δ are also used to find the activation energy E [18]. It is noted that Eq. (11) describes IMTS TL peaks in an accurate manner, without approximations and errors other than those due to the numerical resolution used for the temperature evaluation during the simulation.

The results for E and b obtained using the above two methods of analysis, were also verified by fitting the numerically generated TL peaks using several computerized fitting algorithms. These computerized algorithms are based on the empirical GO Eq. (1) and will be presented elsewhere, since they are beyond the scope of this paper. The important point as far as this paper is concerned, is that these computerized curve fitting methods of analysis agreed within 1% or better, with the results obtained using the two peak shape methods described above.

3 Results

3.1 Dependence of T_{\max} and b on the irradiation dose: The OTOR model The OTOR model is described by the set of Eqs. (2)–(7) with $A_d = 0$, and the simulated shift of T_{\max} versus dose resulting from this model is shown in Fig. 1.

The upper part of Fig. 1 shows the simulated shift of T_{\max} as a function of the ratio of retrapping and recombination coefficients A_r/A_m in the OTOR model. Several curves are shown for variable trap fillings n_o/N which represent the prior irradiation dose to the sample. In all cases shown in Fig. 1, the recombination coefficient has a fixed value of $A_m = 10^{-7} \text{ cm}^3/\text{s}$. This behavior predicted by the OTOR model is very similar to the results obtained using the analytical expressions for GO kinetics Eq. (1) (see, e.g., [2, 3]). By using the values of T_{\max} and the known E , the effective kinetic order parameter b was evaluated in this model using either Eq. (11), or directly from the geometrical factor μ_g .

The results of these evaluations are shown in the lower Fig. 1, which shows b as a function of A_r/A_m , and for several trap fillings n_o/N . As in the case of the analytical GO expressions, the shift of T_{\max} with dose in the OTOR model, is accompanied by a strong variation of the effective kinetic order b . The only exception is the case of first-order kinetics, in which $b = 1$ and $T_{\max} = \text{constant} = 385 \text{ K}$ at all trap fillings n_o/N .

The conditions under which the OTOR model can lead to first-order and second-order kinetics have been discussed in detail in the literature (see, e.g., Ref. [12]). If $A_n m \gg A_r (N - n)$, and if $dm/dt = dn/dt$, one gets the first-order equation in the OTOR model; this condition includes

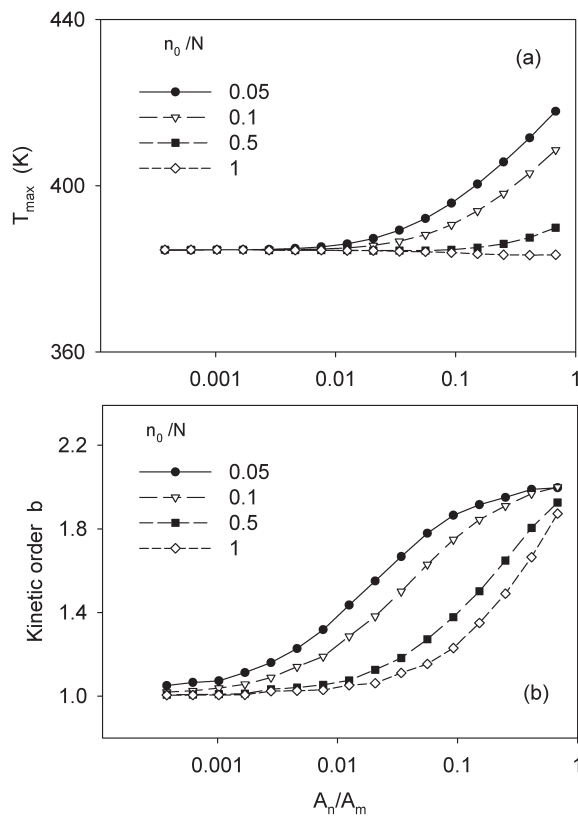


Figure 1 Simulation results in the OTOR model. Upper figure: Simulation of the shift of T_{\max} as a function of the ratio of retrapping and recombination coefficients A_n/A_m . In all cases shown in this figure, the recombination coefficient $A_m = 10^{-7} \text{ cm}^3/\text{s}$. (b) The effective kinetic order as a function of A_n/A_m for various trap occupancies n_0/N .

A_m , A_n , N , m , and n . The second-order case can be obtained from the OTOR equations in one of two possible ways. In the first case the conditions $A_n(N - n) \gg A_m m$ along with $N \gg n$ and $m = n$ must hold. In the second case one obtains the second-order kinetics equations by using the more restrictive conditions $A_m = A_n$ and $m = n$.

However, there is an additional situation in which the OTOR model results in first-order kinetics, namely when $A_n/A_m \rightarrow 0$. Figure 1 represents an example of what happens to the OTOR results when the QE conditions hold and $A_n/A_m \rightarrow 0$, that is, when retrapping becomes negligible compared to recombination. In this case, the OTOR model results in first-order kinetics, no matter what the values of the other parameters in the model. The two conditions discussed here, namely $A_m m \gg A_n(N - n)$ and $A_n/A_m \rightarrow 0$ are nearly the same, with the former resulting from the latter.

The numerical TL peaks generated by the OTOR model were analyzed, and the value of the activation energy E was calculated using Eq. (9), or alternatively from Eq. (11). The results from this analysis show a deviation of less than 5% from the expected value of $E = 1 \text{ eV}$ in all studied cases, indicating that this parameter can be extracted with

confidence from the OTOR glow curves, at least within this accuracy.

These results are in agreement with the previous simulations carried out by Sunta et al. [2, 3], and are discussed in more detail in a subsequent section with regards to the IMTS model.

The conclusion of this section is that the OTOR model predicts a shift of T_{\max} , a variation of the effective kinetic order parameter b , and a change in the shape of glow curves with the irradiation dose.

These theoretical predictions of the OTOR model have never been verified convincingly by experiment. The simulations also show that the activation energy E can be extracted accurately within a few percent from the numerically generated OTOR peaks, by using GO expressions.

3.2 Dependence of T_{\max} and b on the irradiation dose: The IMTS model The key element of the IMTS model is the existence of competition between the two traps and the center during the TL heating stage.

There are several types of competition processes taking place simultaneously in the model, and their importance depends on the relative values of the retrapping and recombination coefficients A_m , A_n , and A_d . The first type of competition is between the retrapping and recombination coefficients A_n and A_m ; higher values of A_n will lead to more retrapping, and hence to a smaller TL signal, while higher A_m values will lead in general to a higher TL signal. The second type of competition is between the capture coefficient A_d of the competitor trap, and the coefficients A_n and A_m ; higher values of A_d will remove electrons from the conduction band, and this will lead to a smaller TL signal. The third type of competition is due to the relative initial concentrations of charge carriers in the dosimetric trap n_{10} and in the competing trap n_{20} .

We start with a systematic study of how the three retrapping and recombination probabilities A_m , A_n , A_d affect T_{\max} and the effective kinetic order parameter b .

Figure 2(a) shows the effect of varying the retrapping coefficient A_n of the dosimetric trap, on the effective kinetic order b . Figure 2(b) shows the corresponding results for T_{\max} . Several sets of simulated data are shown, for different dosimetric trap fillings n_{10}/N_1 . As the retrapping coefficient A_n is *decreased*, all curves tend to first-order kinetics $b = 1$ and to the corresponding expected constant value of $T_{\max} = 385 \text{ K}$ at all doses. This result makes physical sense, since very small retrapping in the dosimetric trap should lead to first-order kinetics.

Figure 3 shows the effect of varying the retrapping coefficient A_d of the competitor trap on b and for different dosimetric trap fillings n_{10}/N_1 . In this case the effect is the exact opposite of the effect shown in Fig. 3; as the retrapping coefficient for the competitor A_d is *increased*, all curves tend to first-order kinetics $b = 1$. This result indicates that strong retrapping probability into the competitor trap can also lead to first-order kinetics behavior.

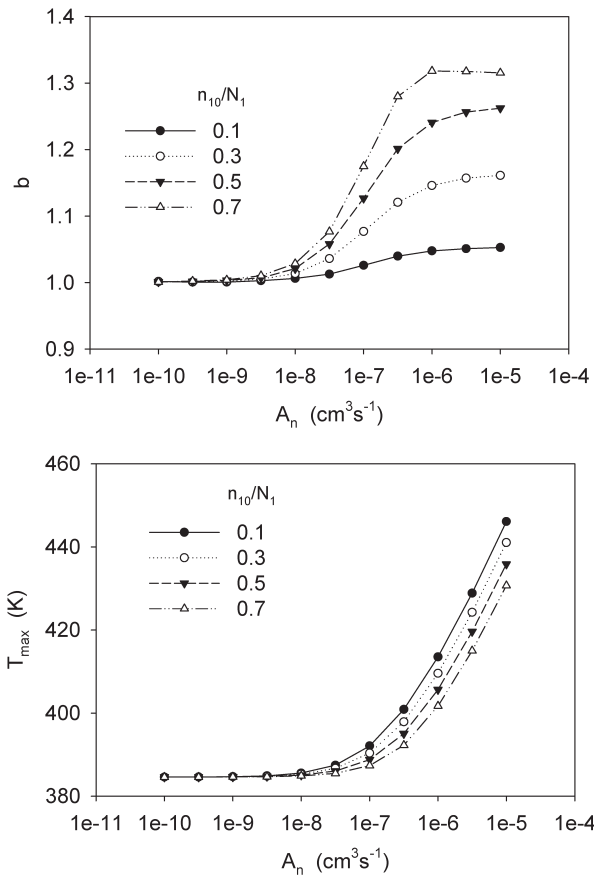


Figure 2 Simulation results from the IMTS model. The effect of varying the retrapping coefficient A_n of the dosimetric trap, on the effective kinetic order b (upper figure), and on T_{\max} (lower figure). Several sets of simulated data are shown, for different dosimetric trap fillings n_{10}/N_1 .

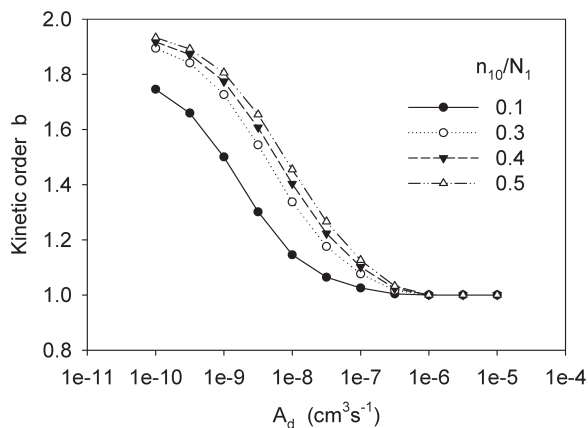


Figure 3 Simulation results from the IMTS model. The effect of varying the retrapping coefficient A_d of the competitor trap, on the effective kinetic order b . Several sets of simulated data are shown, for different dosimetric trap fillings n_{10}/N_1 .

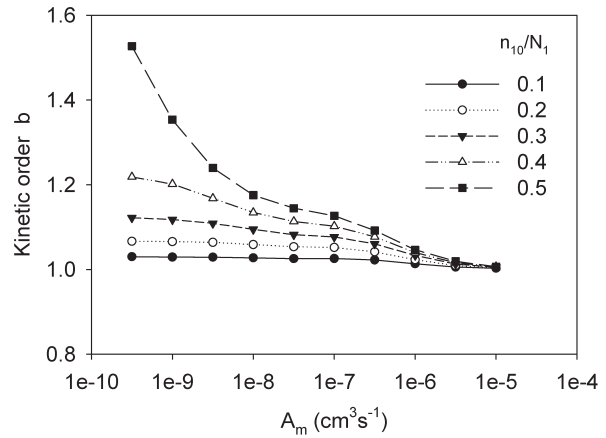


Figure 4 Simulation results from the IMTS model. The effect of varying the recombination coefficient A_m in the IMTS model, on the effective kinetic order b . Several sets of simulated data are shown, for different dosimetric trap fillings n_{10}/N_1 .

Figure 4 shows the effect of varying the recombination coefficient A_m , on the values of b . Here the effect is similar to the situation shown in Fig. 3; as the recombination coefficient A_m is increased, all curves tend to first-order kinetics $b = 1$.

Figure 5 shows the effect of varying the total concentration N_2 of the competitor trap. Here, the effect is also identical to the situation in Fig. 3, with higher competitor concentration N_2 leading to first-order kinetics $b = 1$ for all initial concentrations n_{10} . This can be understood mathematically from the term $n_c(N_2 - n_2)A_d$ in Eq. (5), which increases with N_2 , leading to higher retrapping in the competitor trap.

The main conclusion from Figs. 2–5 is that stronger retrapping into the competitor trap will tend to favor first-order kinetics, and consequently the shape of TL glow curves

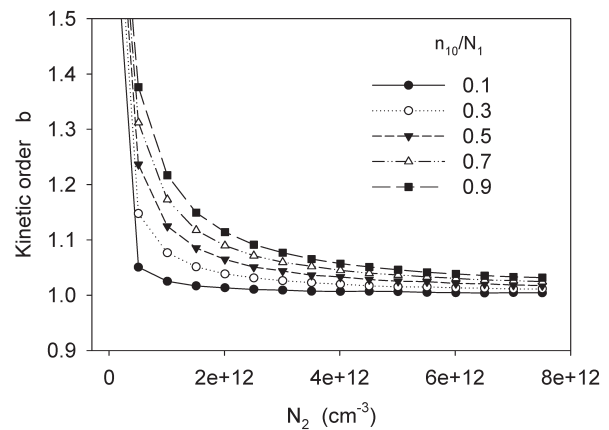


Figure 5 Simulation results from the IMTS model. The effect of varying the total concentration N_2 of the competitor trap, on the effective kinetic order b . Several sets of simulated data are shown, for different dosimetric trap fillings n_{10}/N_1 .

would remain the same at all doses, as observed in most dosimetric materials. In the next two sections we pursue this idea of a correlation between strong retrapping in the competitor traps and first-order kinetics further, by simulating the average behavior of dosimetric materials.

3.3 Simulation of the average behavior of dosimetric materials using the IMTS model In a real dosimetric material one can expect random variations of the recombination/retrapping coefficients A_m, A_n, A_d as well as random variations in the concentrations of the traps N_1, N_2, n_{10} , and n_{20} appearing in the IMTS model. Such random variations would lead to statistical variations between different samples of the same material, and even in significant differences between different aliquots of the same sample. We simulate the random natural variations of the coefficients A_m, A_n , and A_d and of the initial concentrations n_{10} and n_{20} , by allowing these parameters to vary between physically reasonable minimum and maximum values.

Unfortunately the coefficients A_m, A_n , and A_d have been measured for only a few dosimetric materials [22]. However, their range is believed to be as low as 10^{-10} cm³/s and as high as 10^{-5} cm³/s [12, 23]. Since these values represent a span of 5 orders of magnitude, we allow random uniform variations in their *logarithms*, rather than in the values themselves [24].

Similarly, we allow the logarithms of the trap fillings n_{10} and n_{20} for the dosimetric trap and the competitor correspondingly, to vary from a low value of $0.01N_1$ and $0.01N_2$ (1% filled traps), to a high value of $0.99N_1$ and $0.99N_2$ (99% filled traps). These five parameters A_m, A_n, A_d, n_{10} , and n_{20} were varied randomly within the above broad physical limits. The total trap concentrations N_1 and N_2 were kept constant at $N_1 = N_2 = 10^{12}$ cm⁻³, in order to avoid numerical instabilities which can occur when using extremely large ranges for the randomly varying parameters in the model. This choice of constant N_1, N_2 values does not affect the results of the simulation, since the properties of importance are the trap filling ratios n_{10}/N_1 and n_{20}/N_2 , rather than the absolute values of N_1 and N_2 . The kinetic parameters E, s characterize the TL trap, and are also kept fixed at $E = 1$ eV and $s = 10^{12}$ /s, as in the previous simulations in this paper.

Figure 6 shows the results of simulating $N = 1000$ random variants of the IMTS model, produced in the above manner.

Figure 6(a) shows the simulated distribution of T_{\max} , with a mean value of (402 ± 30) K (1σ). This mean value is relatively close to the value expected for first-order kinetics, $T_{\max} = 385$ K, as discussed above. Figure 6(b) shows the corresponding distribution of the effective kinetic order parameter b , with a mean value of (1.08 ± 0.16) (1σ). Similarly, Fig. 7 shows the distribution of the geometrical shape factor μ_g with a mean value of (0.43 ± 0.03) (1σ), and the distribution of energies E_g with a mean value of (0.98 ± 0.10) eV (1σ).

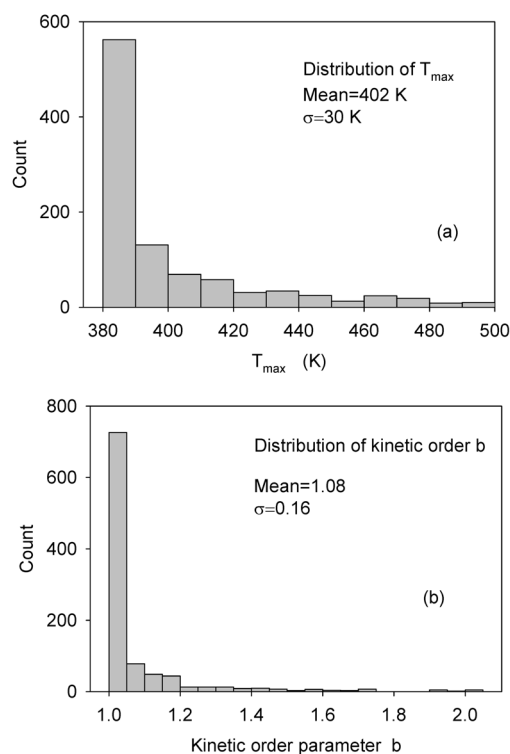


Figure 6 Simulation of $N = 1000$ random variants of the IMTS model, as described in the text. The upper figure shows the distribution of T_{\max} , and the lower figure the distribution of effective kinetic order b .

The overall results shown in Figs. 6 and 7 are rather remarkable. They indicate strongly that the average position and average shape of the TL glow peak is determined almost exclusively by the parameters E and s . Random variations of the five parameters A_m, A_n, A_d, n_{10} , and n_{20} within many orders of magnitude, have little effect on the average shape and position of the glow peak. Furthermore, first-order kinetics is clearly preferred statistically over higher order kinetics, as seen in the histogram of Fig. 6(b).

These simulated results were verified by running the simulation with $N = 10^4$ random variants of the model. This resulted in a small change of the order of 1% or less in the average values of the parameters, and in little apparent change of the overall shape of the histograms. The main result of using more natural variants in the simulation was mostly to “smooth out” and to narrow the histograms, by reducing the standard deviation of the results; this is to be expected due to the improvement in statistics, resulting from using more points in the simulations. The resulting reduction of the calculated standard deviations was of the order expected from statistical considerations, with σ varying approximately as $1/\sqrt{N}$. It is concluded that the conclusions drawn from the simulations shown in Figs. 6 and 7 are independent of the number of natural variants N used in the simulations.

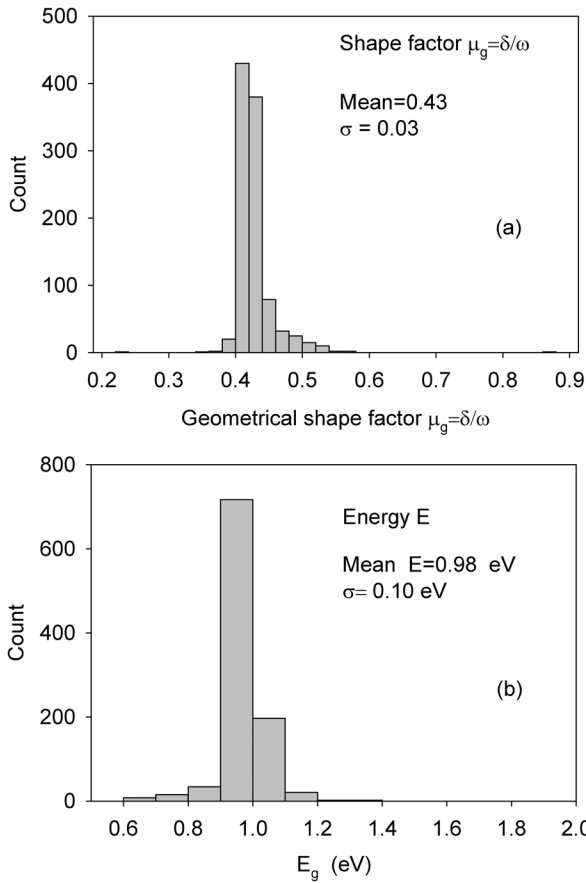


Figure 7 Simulation of $N=1000$ random variants of the IMTS model, as described in the text. Upper figure: The distribution of the geometrical shape factor μ_g . Lower figure: The distribution of energies E_g calculated using GOK.

Previous authors [2, 25, 26] used a much more limited range of kinetic parameters than the wide ranging values used in the present simulations. As a result, they drew their conclusions based on a few simulations within the IMTS model. The main advantage of the new method proposed in this paper, is that the average behavior of a natural material can be simulated more accurately, and for a very wide range of the kinetic parameters.

Figure 8 shows the effective kinetic order b as a function of the trap filling ratio n_{10}/N_1 for the $N=1000$ variants of the model. The simulation in Fig. 8 has been extended to very low values of the trap filling ratio, as low as $n_{10}/N_1 = 10^{-6}$, to show the effect of low trap filling ratios more clearly. These simulated data show that as the trap filling becomes very small, the TL glow curves tend systematically toward first-order kinetics $b = 1$. This result is consistent with the previous suggestion of Sunta et al. [27], who investigated and summarized the conditions under which first-order TL glow peaks are produced within a generalized IMTS model. One of their important conclusions was that simulated TL glow always become of first-order at low trap occupancies. On the basis of this general conclusion, these authors recommended

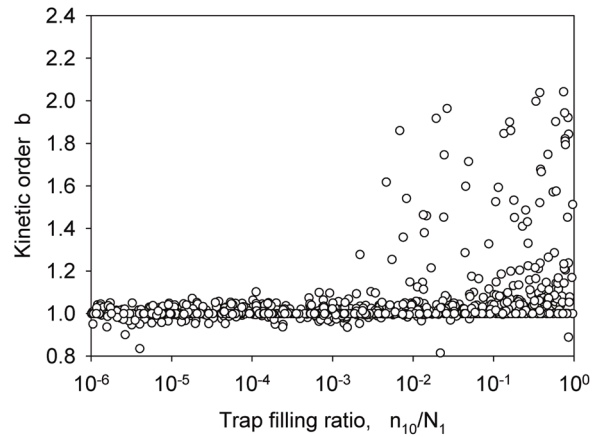


Figure 8 Correlation of effective kinetic order parameter b with the initial trap filling ratio n_{10}/N_1 . Simulation results are shown from $N=1000$ variants of the IMTS model.

that analysis of TL glow curves should always be carried at low irradiation doses.

3.4 Effect of the presence of additional competitors on T_{max} and b The results of the previous sections lead us to investigate systematically the effect of additional trapping levels in the IMTS model. Specifically we systematically add increasing number of thermally disconnected traps with instantaneous and total concentrations n_i and N_i correspondingly, and with re trapping coefficients A_i ($i = 1 \dots 12$). Each one of these levels will satisfy a differential equation of the form

$$\frac{dn_i}{dt} = n_c(N_i - n_i)A_i, \quad (12)$$

and these equations are added to the system of differential Eqs. (2)–(7) in this paper. The charge conservation Eq. (7) is also modified appropriately each time a trapping level is added, to account for the additional charge introduced in the model.

Figure 9 shows a simulation of T_{max} for $N=1000$ random variants of the IMTS model, and for an increasing number of competitors $M=2$ and 12. As the number M of competitor traps increases, the histogram distribution of the $N=1000$ random variants becomes more narrow, and the average value in the histogram tends toward the expected value of $T_{max} = 385$ K for first-order kinetics. The corresponding mean values of T_{max} for $M=1, 2, 12$ are (402 ± 30) K, (396 ± 22) K, and (386 ± 3) K (1σ).

Figure 10 shows the corresponding results for the effective kinetic order b . In all of these results, the histograms become progressively narrower as M increases, and the average values of the distribution approach the expected first-order kinetic values. The mean value of b for $M=1, 2, 12$ competitors are (1.08 ± 0.16) , (1.02 ± 0.08) , and (1.005 ± 0.016) (1σ). The corresponding values of energy

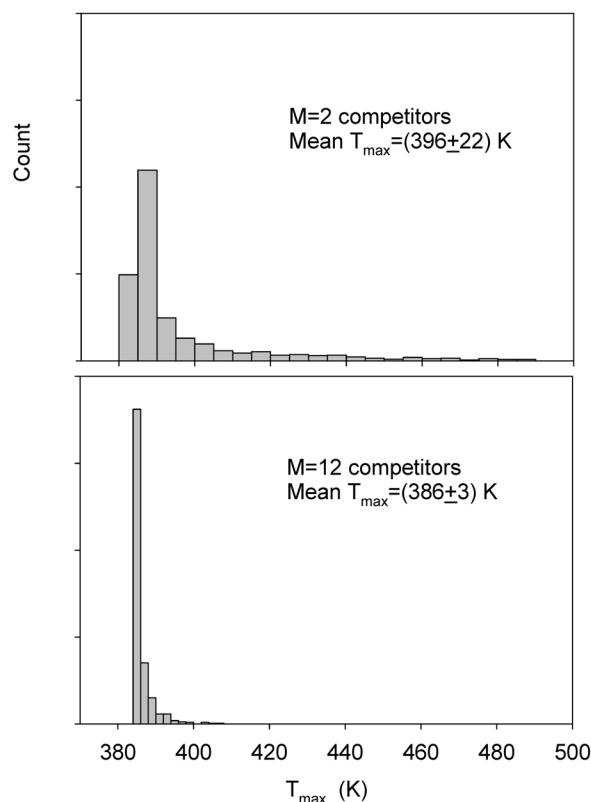


Figure 9 Simulation of T_{\max} for $N = 1000$ random variants of the IMTS model and for increasing number M of competitors, as described in the text. Two cases are shown, for $M = 2$ and 12. As the number of competitors M is increased, the distribution of T_{\max} becomes more narrow, and the average value tends toward the value of $T_{\max} = 385$ K for first-order kinetics.

E_g calculated using GO kinetics are (0.98 ± 0.10) eV for $M = 1$ competitor trap, and (1.004 ± 0.025) eV for $M = 12$ competitor traps.

These simulated results are summarized more clearly in Figs. 11 and 12, which show the overall effect of increasing the number of competitors M on the effective kinetic order b , on T_{\max} , on E , and on the geometrical shape factor μ_g . As the number of competitor traps M increases, the average behavior of the TL glow peaks approaches progressively first-order kinetics, and the simulated results represent progressively better the behavior of real dosimetric materials.

We have repeated the simulation in Figs. 6–12 by including an irradiation stage followed by a relaxation period, and by the heating stage of TL. At the start of the irradiation stage the traps and centers are considered to be empty, that is, the initial concentrations are taken as $n_{10}/N_1 = n_{20}/N_2 = 0$. The results of these simulations were very similar to Figs. 6–12. For example, the mean value of the parameters in the new simulations for $N = 1000$ variants are $b = (1.14 \pm 0.26)$, $T_{\max} = (407 \pm 36)$ K, $E_g = (0.98 \pm 0.06)$ eV, for $M = 1$ competitor traps. The results of these simulations for a variable number of

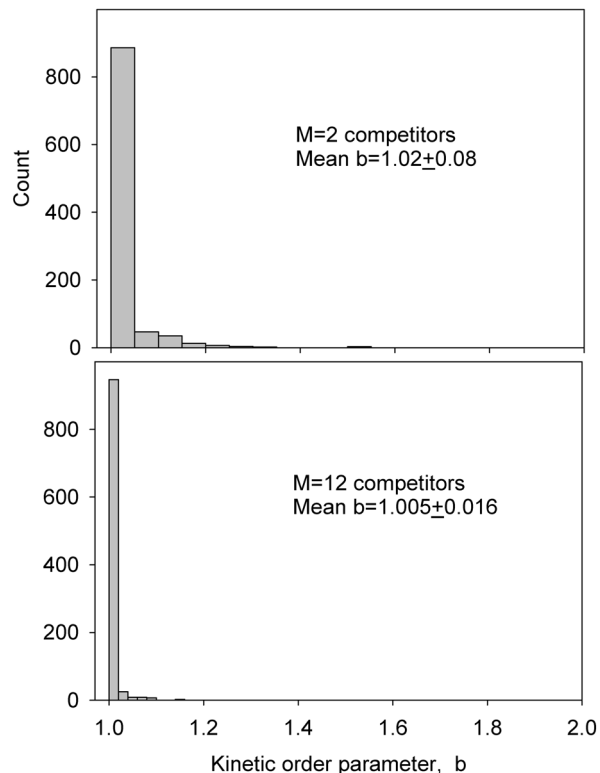


Figure 10 Simulation of the kinetic order b for $N = 1000$ random variants of the IMTS model and for increasing number M of competitors, as described in the text. Two cases are shown, for $M = 2$ and 12.

competitors M were also very similar to Figs. 6–12, with the histograms becoming progressively narrower as M increases, and with the average values of the distributions approaching the expected first-order kinetic values. The overall conclusions from the simulations remain unchanged when these three-stage simulations are carried out.

4 Discussion

4.1 Experimental considerations: Measurements of T_{\max} and b in complex TL glow curves

Sunta et al. [21, 27] posed clearly the central question addressed by this paper: “The question then arises why is first-order prevalent in TL emission? The answer on the basis of the results and discussions in the preceding pages appears to be the following: it is because (i) the QE condition may always be satisfied as discussed earlier; (ii) there is an abundance of TDDTs in the temperature range in which the TL glow peaks are usually recorded.”

In this discussion section we consider these statements, and also discuss several additional topics which are directly relevant to the subject of this paper.

From an experimental point of view, a shift of T_{\max} can be detected rather easily, even in complex TL glow curves. On the other hand, the variation of the effective kinetic order b is very difficult to detect experimentally. The reason is purely experimental, and depends on the accuracy of

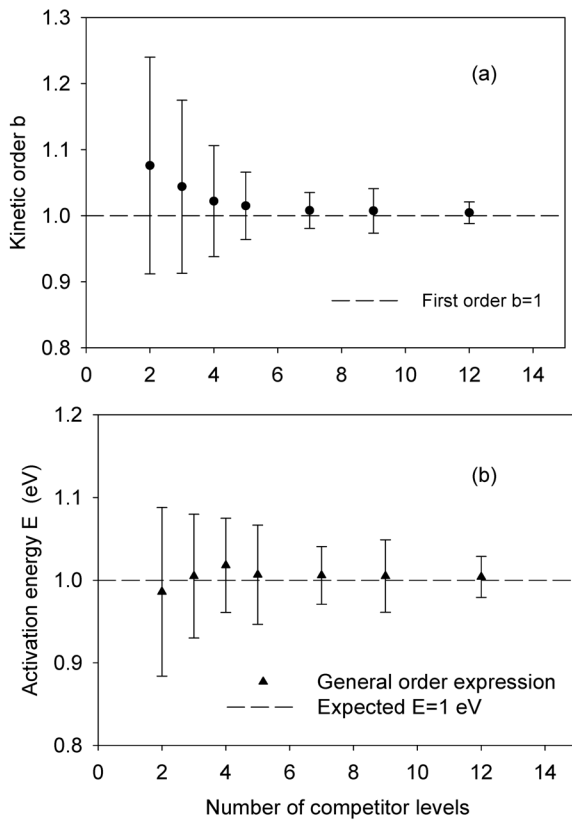


Figure 11 Simulation of the effect of increasing the number of competitors M , on the kinetic order b (upper figure) and on the activation energy E (lower figure), using GO expressions.

the temperature measurements during the TL experiment. For example, in practical TL readouts, data collection is performed every 1 or 2 K. Within this experimental temperature resolution, it is impossible to detect variations of the kinetic order parameter b . This was shown by simulation by Pagonis et al. [28]. These authors showed that in order to discriminate a TL glow curve of kinetic order $b = 1.5$ from a TL glow curve with $b = 1.4$ or $b = 1.6$, a temperature resolution of less than 0.2 K is required. This type of experimental temperature resolution and accuracy is difficult, if not impossible, to ensure during a typical TL experiment.

4.2 The effect of competitors on the shape of TL glow curves The simulation results in this paper show clearly the effect of the retrapping/recombination coefficients on the apparent kinetic order. Specifically, the simulated data shows a correlation between the strength of the competition and the kinetic order b ; as the competition from other traps becomes more important, the system tends toward first-order kinetics. Stated simply, the stronger the competition, the lower the kinetic order b , and therefore the smaller the shift of T_{\max} at different doses. This simple statement offers a possible explanation of why a shift of T_{\max} is not observed experimentally at different doses.

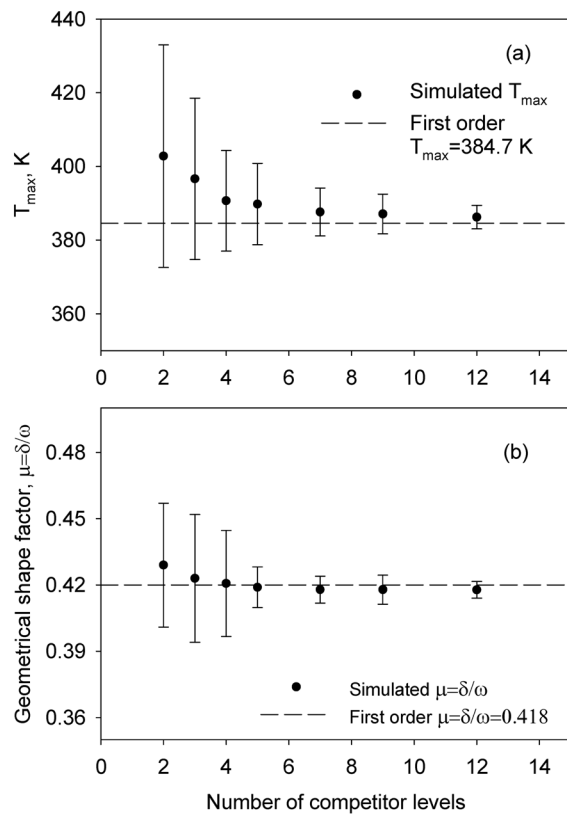


Figure 12 Simulation of the effect of increasing the number of competitors M , on T_{\max} (upper figure), and on the geometrical shape factor (lower figure).

In a real dosimetric system there are many energy levels, and strong competition with the luminescence process is always present, leading to first-order kinetics for most materials [4].

From a physical point of view, broad TL peaks and high T_{\max} values are obtained when the recombination rate is very weak so that recombination events are dispersed over a longer range of temperatures during the heating stage. Thermally released carriers can be retrapped and re-emitted a very large number of times before recombining, producing a broad TL peak with a high T_{\max} . This effect of deep traps on the shape of glow curves has been simulated by Mady et al. [29]. In general, any mechanism that can extract carriers permanently from the conduction band will suppress the late recombination events and the intensity of the high temperature side of the TL peak is decreased, leading to an apparent first-order shape of the TL glow curve.

4.3 Alternative explanations for the prevalence of first-order TL kinetics Bos [1] reviewed the applicability of the first-order Randall–Wilkins model, and examined its underlying assumptions, namely the QE conditions, and the absence of retrapping. The author points out that according to the work of Lewandowski and McKeever [30], first-order kinetics is the only case in which

these two assumptions are self-consistent. Bos [1] also listed several other possible luminescence processes which can lead to first-order kinetics. In the first example of such physical processes, the trap and the center are created close to each other, and recombination takes place from an excited state of the electron into the recombination center. Under certain simplifying assumptions, this type of localized transition can be described by first-order kinetics and seems to be quite common in TL materials [12].

Hence, in this alternative explanation, the prevalence of first-order kinetics can be explained by the existence of trap-luminescence center complexes in close physical proximity in the crystal, leading to localized transitions.

A second possible process which can lead to first-order kinetics, is by simultaneous thermal release of electrons and holes from their traps, with the holes acting as the recombination center. This type of process can also be accompanied by reactions taking place between different types of defects, and was analyzed by Piters and Bos [31], who found that the simulated glow curves follow closely first-order kinetics. However, Bos [1] points out that in this complex situation the fitting parameters E and s cannot be interpreted as the trap activation energy and the escape frequency correspondingly. In practice it is found that complex TL glow curves such as the one for the very popular material LiF:Mg,Ti (TLD-100), can be analyzed by the sum of several first-order TL peaks. However, the fitting parameters do not yield the correct thermal fading properties of the various peaks in this material; this again shows that the fitting parameters cannot be directly interpreted in terms of the kinetic properties of the TL traps.

The main conclusion from this paper is that strong competition effects during the TL heating process can lead to first-order kinetics. This observation is very likely related to the low luminescence efficiency η of dosimetric materials, which is discussed next.

4.4 The low intrinsic luminescence efficiency of dosimetric materials Bos [1, 4, 13] examined the intrinsic TL efficiency η , which is defined as the ratio of the energy emitted as light during TL, to the energy absorbed during the ionizing radiation process. The author reviewed the literature and analyzed the luminescence efficiency of TL materials, by examining several distinct steps in the luminescence production. These steps include the production of electron–hole pairs, trapping of charge, charge transfer processes, and recombination and emission processes.

The efficiency of known TL materials was tabulated, and it was shown to be relatively low, even in the cases of very bright TL materials. The following expression expresses the intrinsic luminescence efficiency [1]:

$$\eta_i = \frac{h\nu}{\beta E'_g} \eta_{tr} p S Q n_{esc}, \quad (13)$$

where $h\nu$ is the average energy of the emitted TL photons, η_{tr} the fraction of carriers, that is, captured in traps and

which can be subsequently thermally stimulated, p is probability of charge carriers being released from the traps, and S represents the efficiency of transporting these carriers to the luminescent center. Q is quantum efficiency of photon emission by excitation/de-excitation of the luminescence center. E'_g is the forbidden band gap width, and β is a parameter between 1 and 4, expressing the total energy $\beta E'_g$ required to create an electron–hole pair. Finally, n_{esc} is the fraction of photons that escape the material without being absorbed.

Bos [1] estimated the upper theoretical limit for TL materials, and this was found to be on the average $\sim 13\%$. This constancy of the luminescence efficiency was attributed to the fact that most of the energy is lost in the first step, that is, during creation of electron–hole pairs. Other factors which can influence the actual amount of luminescence energy are the thermal quenching effect, concentration quenching, and optical transparency of the material [1].

The author concluded that the trapping efficiency plays a dominant role in the overall intrinsic luminescence efficiency of TL materials. Moreover, in many cases the efficiency η of real materials is lower than the theoretical upper limit of 15% by a factor of 300–400. If one assumes that this extra factor of 300–400 is shared equally between the irradiation and recombination stages of TL, then it is possible that several of the parameters appearing in Eq. (13) could be of the order of 1%.

Therefore, the trapping and thermal release of electrons is by its nature a low probability effect [4]. If the luminescence efficiency during the recombination stage is of the order of 1–5%, then 95–99% of the total energy deposited must be lost to other unknown non-radiative processes. These alternative pathways would play the equivalent role to the competing deep traps simulated in this paper, and their presence would also lead to first-order kinetics.

5 Conclusions In this paper, the shift of T_{max} with the irradiation dose was simulated using analytical TL expressions, as well as several TL models of increasing complexity. The simulation results showed that the shift of T_{max} as a function of dose is always accompanied by a variation of the kinetic order.

The simulated changes of T_{max} and of the kinetic order b depend strongly on the strength of the competitor processes, as was shown in Figs. 3–6. The stronger the competition to the luminescence process, the lower the kinetic order b , and therefore the smaller the observed shift of T_{max} with the irradiation dose.

In real physical systems consisting of many trapping levels, the competition to the luminescence process will be very strong. This causes the TL peaks to be mainly of first or near first-order kinetics, and therefore changes to T_{max} cannot be observed easily or accurately during experimental work. This strong competition effect provides a possible explanation of why nature seems to favor first-order kinetics in TL processes. In a real dosimetric system,

these competition effects also correlate to the low luminescence efficiency of dosimetric materials, both during the irradiation and during the recombination stage of TL.

The simulations in this paper provide strong support for the assertion of previous authors, that the abundance of competitor traps in a real dosimetric material “forces” the behavior of these materials toward first-order kinetics. It is noted that the results in this paper do not exclude the possibility of observing GO kinetics behavior in TL materials, but rather provide a demonstration of the reasons why first order is *prevalent* in TL processes, as opposed to GO kinetics which is rarely observed experimentally.

References

- [1] A. J. J. Bos, *Radiat. Meas.* **41**, S45 (2007).
- [2] C. M. Sunta, W. E. Ayta, T. M. Piters, and S. Watanabe, *Radiat. Meas.* **30**, 197 (1999).
- [3] C. M. Sunta, W. E. Ayta, J. F. D. Chubasi, and S. Watanabe, *Radiat. Meas.* **35**, 47 (2002).
- [4] A. J. J. Bos, *Radiat. Meas.* **33**, 737 (2001).
- [5] J. T. Randall and M. H. F. Wilkins, *Proc. R. Soc. Lond. A* **184**, 390 (1945).
- [6] G. F. J. Garlick and A. F. Gibson, *Proc. Phys. Soc. Lond.* **60**, 574 (1948).
- [7] W. Hoogstraaten, *Philips Res. Rep.* **13**, 515 (1958).
- [8] R. Chen and A. Winer, *J. Appl. Phys.* **41**, 5227 (1970).
- [9] R. Chen, *J. Appl. Phys.* **40**, 570 (1969).
- [10] R. Chen, *J. Electrochem. Soc.* **116**, 1254 (1969).
- [11] R. Chen and Y. Kirsh, *Analysis of Thermally Stimulated Processes* (Pergamon, Oxford, 1981), p. 167.
- [12] R. Chen and S. W. S. McKeever, *Theory of Thermoluminescence and Related Phenomena* (World Scientific, Singapore, 1997).
- [13] A. J. J. Bos, *Nucl. Instrum. Methods Phys. Res. B* **184**, 3 (2001).
- [14] C. E. May and J. A. Partridge, *J. Chem. Phys.* **40**, 1401 (1964).
- [15] M. Rasheedy, *J. Phys.: Condens. Matter* **5**, 633 (1993).
- [16] P. W. Levy, *Nucl. Tracks Radiat. Meas.* **10**, 21 (1982).
- [17] G. Kitis, R. Chen, and V. Pagonis, *Phys. Status Solidi A* **205**, 1181 (2008).
- [18] G. Kitis and V. Pagonis, *Nucl. Instrum. Methods Phys. Res. B* **262**, 313 (2007).
- [19] B. Subedi, G. Kitis, and V. Pagonis, *Phys. Status Solidi A* **207**, 1216 (2010).
- [20] A. Halperin and A. A. Braner, *Phys. Rev.* **117**, 408 (1960).
- [21] C. M. Sunta, W. E. F. Ayta, J. F. D. Chubaci, and S. Watanabe, *J. Phys. D* **38**, 95 (2005).
- [22] M. Lax, *Phys. Rev.* **119**, 1502 (1960).
- [23] R. Chen and V. Pagonis, *Thermally and Optically Stimulated Luminescence: A Simulation Approach* (John Wiley and Sons, Chichester, 2011).
- [24] G. Adamiec, M. Gracia-Talavera, R. Bailey, and P. Iniguez de la Torre, *Geochronometria* **23**, 9 (2004).
- [25] C. M. Sunta, W. E. F. Ayta, R. N. Kulkarni, T. M. Piters, and S. Watanabe, *Radiat. Prot. Dosim.* **84**, 25 (1999).
- [26] C. M. Sunta, W. E. F. Ayta, J. F. D. Chubaci, and S. Watanabe, *Radiat. Prot. Dosim.* **84**, 51 (1999).
- [27] C. M. Sunta, W. E. F. Ayta, J. F. D. Chubaci, and S. Watanabe, *J. Phys. D* **34**, 2690 (2001).
- [28] V. Pagonis, G. Kitis, and C. Furetta, *Numerical and Practical Exercises in Thermoluminescence* (Springer, New York, 2006), p. 76.
- [29] F. R. Mady, R. Bindi, P. Iaconi, and F. Wrobel, *Radiat. Prot. Dosim.* **119**, 37 (2006).
- [30] A. C. Lewandowski and S. W. S. McKeever, *Phys. Rev. B* **43**, 8163–8178 (1991).
- [31] T. M. Piters and A. J. J. Bos, *J. Phys. D* **27**, 1747 (1994).